

Mixed aza–thia crowns containing the 1,10-phenanthroline sub-unit. Substitution reactions in $[\text{NiL}(\text{MeCN})][\text{BF}_4]_2$ $\{\text{L} = 2,5,8\text{-trithia}[9](2,9)\text{-}1,10\text{-phenanthroline}\}^\dagger$

Alexander J. Blake,^a Jaume Casabò,^b Francesco A. Devillanova,^{*c} Lluís Escriche,^b Alessandra Garau,^c Francesco Isaia,^c Vito Lippolis,^{*c} Raikko Kivekas,^d Vincens Muns,^b Martin Schröder,^a Reijo Sillanpää^e and Gaetano Verani^c

^a School of Chemistry, University of Nottingham, Nottingham, UK NG7 2RD

^b Departament de Química (Unit Inorganica), Universitat Autònoma de Barcelona, 08193 Bellaterra, Barcelona, Spain

^c Dipartimento di Chimica e Tecnologie Inorganiche e Metallorganiche, Università degli Studi di Cagliari, Via Ospedale 72, 09124 Cagliari, Italy.
E-mail: lippolis@vaxca1.unica.it

^d Department of Chemistry, University of Helsinki, PO Box 55, FIN 00014 Helsinki, Finland

^e Department of Chemistry, University of Turku, FIN-20500 Turku, Finland

Received 19th October 1998, Accepted 27th January 1999

The substitution reactions of the co-ordinated acetonitrile molecule in $[\text{NiL}(\text{MeCN})][\text{BF}_4]_2$ **1** ($\text{L} = 2,5,8\text{-trithia}[9](2,9)\text{-}1,10\text{-phenanthroline}$) with different anionic and neutral ligands L' [Cl^- , Br^- , I^- , CN^- , SCN^- , H_2O , pyridine (py), aniline (an), 1,3-dimethyl-4-imidazoline-2-thione (etu) or 1,3-dimethyl-4-imidazoline-2-selone (eseu)] have been studied by using electronic spectroscopy. While the reaction with all the anionic ligands is quantitative, for the neutral ones an equilibrium takes place; the corresponding equilibrium constants have been determined in MeCN at 25 °C. The complex cations $[\text{NiL}(\text{L}')^{2-n}]^{2-n+}$ ($n = 0$ for neutral and 1 for anionic ligands) have also been isolated in the solid state, mainly as BF_4^- salts and the compounds $[\text{NiL}(\text{H}_2\text{O})][\text{ClO}_4]_2 \cdot \text{H}_2\text{O}$, $[\text{NiL}(\text{Cl})\text{Cl} \cdot \text{H}_2\text{O}$, $[\text{NiL}(\text{SCN})]\text{-BF}_4 \cdot \text{MeNO}_2$, $[\text{NiL}(\text{eseu})][\text{BF}_4]_2$ and $[\text{NiL}(\text{py})][\text{BF}_4]_2$ have been characterized by X-ray diffraction studies. In these complexes a distorted octahedral geometry is achieved at the Ni^{II} with five sites occupied by the macrocyclic ligand L and the sixth by the appropriate ligand L' . The electrochemistry of all the prepared compounds has been studied by cyclic voltammetry. In particular the reductive cyclic voltammetry of **1** in acetonitrile shows a quasi-reversible one-electron reduction wave near $^1E_1 = -1.0$ V vs. Fc/Fc^+ . Electrochemical reduction by controlled-potential electrolysis at this potential in the presence of the axial ligand PMe_3 , and investigation of the reduced product by ESR spectroscopy confirm the reduction process to be metal based and to correspond to the formation of the $[\text{Ni}^{\text{I}}\text{L}]^+$ species.

Introduction

The chemical and structural features of macrocyclic metal complexes can be tuned by incorporating different soft and hard donor atoms in the chelating ring, thereby promoting the stabilization of both low and high oxidation states of the metal centre, as well as forcing metal ions to adopt an atypical coordination geometry. In this context, thia¹ and mixed aza–thia² crown ethers have been the subject of intense interest in the last few years, particularly as their complexes are useful model compounds for biological systems.³

Furthermore, the presence in the macrocyclic framework of rigid heterocyclic molecules such as pyridine (py), 2,2'-bipyridine (bipy) and 1,10-phenanthroline (phen), which carry hard N-donor atoms and are excellent π acceptors, has been shown to both stabilize low-valent metal complexes and to have a marked influence on the co-ordination geometry.^{4–6} Interest in the co-ordination chemistry of substituted derivatives of bipy and phen is based mainly on the catalytic, redox and photo-redox properties of some of their metal complexes⁷ as well as

on their use as building blocks for supramolecular devices.⁸ In this context, we have recently reported the synthesis of new mixed aza–thioether crowns incorporating the 1,10-phenanthroline sub-unit and their co-ordinating properties towards Ni^{II} , Pd^{II} , Pt^{II} and Rh^{III} .^{9,10a} In particular, the pentadentate ligand 2,5,8-trithia[9](2,9)-1,10-phenanthroline (L) has been shown to have chelating properties dependent upon the conformational constraints imposed by the phenanthroline unit on the S-donor thioether linker of the ring. For example, the locked [4 + 1] co-ordination sphere that L can impose on Pd^{II} and Pt^{II} , as well as the nature of its donor atom set, seems to be responsible for the stabilization of the corresponding low-valent complexes of Pd^{I} and Pt^{I} .^{10a} In the case of Ni^{II} the crystal structures of the complexes $[\text{NiL}(\text{MeCN})][\text{BF}_4]_2$ **1**, $[\text{NiL}(\text{Cl})]\text{-BF}_4 \cdot \text{dmf}$ **2** and $[\text{NiL}(\text{I})]_3$ **3** have been reported previously.⁹ In these a distorted octahedral geometry is achieved at the metal with five sites occupied by the macrocyclic ligand and the sixth by MeCN , Cl^- or I^- , respectively. The MeCN molecule in **1** can readily be substituted and this offers a good route to prepare different pseudo-octahedral nickel(II) complexes in which the metal centre always remains encapsulated within the co-ordinating cavity imposed by L .

We report herein a study on the substitution reactions of the co-ordinated acetonitrile molecule in complex **1** with different anionic and neutral L' ligands [Cl^- , Br^- , I^- , CN^- , SCN^- , H_2O , pyridine, aniline (an), 1,3-dimethyl-4-imidazoline-2-thione (etu)

[†] Supplementary data available: isobestic points in the titration of **1** with L' . For direct electronic access see <http://www.rsc.org/suppdata/dt/1999/1085/>, otherwise available from BLDSC (No. SUP 57496, 3 pp.) or the RSC Library. See Instructions for Authors, 1999, Issue 1 (<http://www.rsc.org/dalton>).

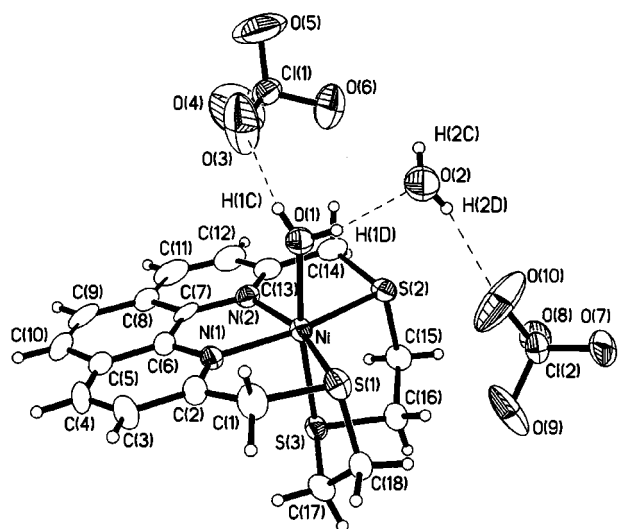
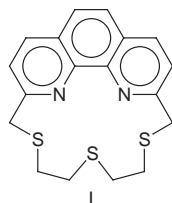
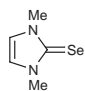
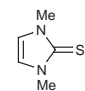


Fig. 1 View of $[\text{NiL}(\text{H}_2\text{O})](\text{ClO}_4)_2 \cdot \text{H}_2\text{O}$ **4** with the numbering scheme adopted. Displacement ellipsoids are drawn at 30% probability.

and 1,3-dimethyl-4-imidazoline-2-selone (eseu)] using electronic spectroscopy. The electrochemical properties of the complexes obtained and the crystal structures of $[\text{NiL}(\text{H}_2\text{O})](\text{ClO}_4)_2 \cdot \text{H}_2\text{O}$ **4**, $[\text{NiL}(\text{Cl})]\text{Cl} \cdot \text{H}_2\text{O}$ **5**, $[\text{NiL}(\text{SCN})]\text{BF}_4 \cdot \text{MeNO}_2$ **6**, $[\text{NiL}(\text{eseu})][\text{BF}_4]_2$ **7** and $[\text{NiL}(\text{py})][\text{BF}_4]_2$ **8** are also described.



L'	$[\text{NiL}(\text{L}')]^{(2-n)+}$	L'	$[\text{NiL}(\text{L}')]^{(2-n)+}$
MeCN	1	Pyridine (py)	8
Cl^-	2, 5	Br^-	9
I^-	3	CN^-	10
H_2O	4	aniline (an)	11
SCN^-	6		
	7		12
(eseu)		(etu)	

$n = 0, 1$

Results and discussion

The strategy adopted in the synthesis of L and the preparation and structural characterization of the complex $[\text{NiL}(\text{MeCN})][\text{BF}_4]_2$ **1**, has been reported previously.⁹ In **1**, L acts as an N_2S_3 -donor encapsulating the metal centre within a cavity having a square-based pyramidal stereochemistry. The MeCN molecule, which completes the octahedral co-ordination sphere, can be replaced by other ligands to give new pseudo-octahedral complexes of type $[\text{NiL}(\text{L}')]^{(2-n)+}$. In this way we prepared $[\text{NiL}(\text{Cl})]\text{BF}_4$ **2**⁹ and $[\text{NiL}(\text{I})]\text{I}_3$ **3**,⁹ and have now synthesized **6–12**, of which $[\text{NiL}(\text{SCN})]\text{BF}_4 \cdot \text{MeNO}_2$ **6**, $[\text{NiL}(\text{eseu})][\text{BF}_4]_2$ **7** and $[\text{NiL}(\text{py})][\text{BF}_4]_2$ **8** have also been characterized by crystal structure determinations. Compounds $[\text{NiL}(\text{H}_2\text{O})](\text{ClO}_4)_2 \cdot \text{H}_2\text{O}$ **4** and $[\text{NiL}(\text{Cl})]\text{Cl} \cdot \text{H}_2\text{O}$ **5** have been obtained directly by treating free L with the appropriate nickel(II) salt (see Experimental section). Figs. 1–3 show the co-ordination sphere around the Ni^{II} and some crystal packing features for the compounds **4**, **5** and **7** respectively and Table 1 summarizes selected bond lengths and angles for all five structurally characterized com-

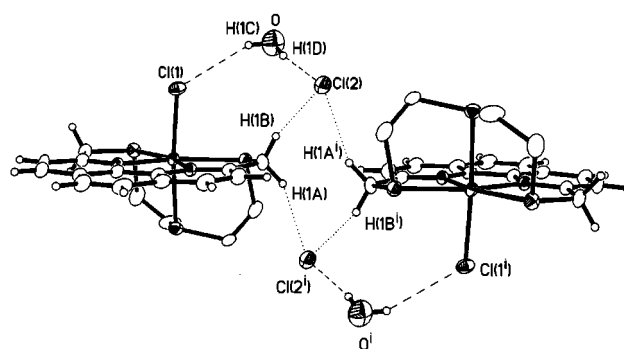


Fig. 2 View of hydrogen-bonded dimeric units in $[\text{NiL}(\text{Cl})]\text{Cl} \cdot \text{H}_2\text{O}$ **5** with the numbering scheme adopted. Displacement ellipsoids are drawn at 30% probability ($i = 3 - x$, $1 - y$, $1 - z$). Only one component of the disordered S-linker of the macrocycle is shown.

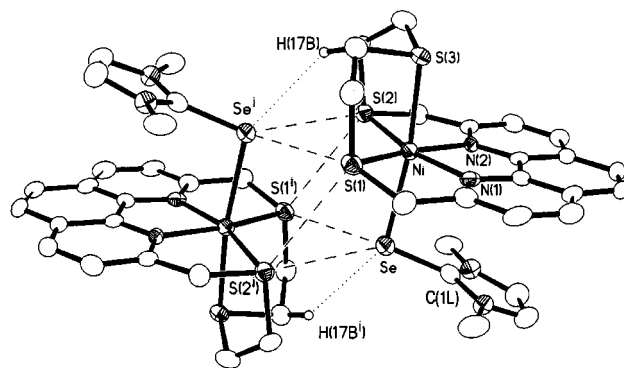


Fig. 3 Dimeric unit of complex cations in $[\text{NiL}(\text{eseu})][\text{BF}_4]_2$ **7** with numbering scheme adopted showing a cubane-like arrangement in the $\text{Ni}_2\text{Se}_2\text{S}_4$ core framework ($i = x$, $1 - y$, $1 - z$). Displacement ellipsoids are drawn at 50% probability, hydrogen atoms have been omitted for clarity.

plexes (the same numbering scheme has been adopted for all the reported structures, see Fig. 1). The nickel(II) ion is bound to the pentadentate macrocycle L via two N-donors of the phen unit, Ni–N ranging from 2.005(12) to 2.041(2) Å, and three thioether S-donors of the thioether linker, Ni–S 2.385(4)–2.481(2) Å (*trans* to phen) and 2.403(5)–2.4445(10) Å (*trans* to L'). The octahedral co-ordination sphere is completed by the neutral or the anionic ligand L' which has replaced the acetonitrile molecule in the starting complex **1**. No significant differences are observed in the conformation adopted by L upon complexation, or in the way it co-ordinates to the metal centre on changing either the counter anion or the nature of the ligand L' which completes the octahedral co-ordination around Ni^{II} . In fact for **2**⁹ and **5** (Fig. 2), which contain the same $[\text{NiL}(\text{Cl})]^+$ complex cation but different counter anions, the bond distances between the metal and the donor atoms of L show variations of the same order of magnitude observed in the other reported complexes (see Table 1), suggesting that solid state effects and the nature of the counter ions are as important as the nature of L' in determining their values. In compound **4** (Fig. 1) the two perchlorate anions form hydrogen bonds with two molecules of water [$\text{H}(1\text{C}) \cdots \text{O}(3)$ 2.08, $\text{H}(1\text{D}) \cdots \text{O}(2)$ 1.96, $\text{H}(2\text{D}) \cdots \text{O}(10)$ 2.23 Å, $\text{O}(1) \cdots \text{H}(1\text{C}) \cdots \text{O}(3)$ 168(8), $\text{O}(1) \cdots \text{H}(1\text{D}) \cdots \text{O}(2)$ 154(8), $\text{O}(2) \cdots \text{H}(2\text{D}) \cdots \text{O}(10)$ 134(10)°] in an *abba* arrangement ($a = \text{ClO}_4^-$, $b = \text{H}_2\text{O}$) with one of the water molecules being co-ordinated to the metal of a $[\text{NiL}]^{2+}$ unit [$\text{Ni} \cdots \text{O}(1)$ 2.089(6) Å, $\text{S}(3) \cdots \text{Ni} \cdots \text{O}(1)$ 172.5(2)°] (Fig. 1). It is interesting that in complex **5** (Fig. 2) the water molecule also bridges the co-ordinated chloride $\text{Cl}(1)$ [$\text{Ni} \cdots \text{Cl}(1)$ 2.3693(10) Å, $\text{S}(3) \cdots \text{Ni} \cdots \text{Cl}(1)$ 169.47(3)°] and the Cl^- counter ion, $\text{Cl}(2)$, through two hydrogen bonds [$\text{Cl}(1) \cdots \text{H}(1\text{C})$ 2.83, $\text{H}(1\text{D}) \cdots \text{Cl}(2)$ 2.33 Å, $\text{Cl}(1) \cdots \text{H}(1\text{C}) \cdots \text{O}$ 152(2), $\text{O} \cdots \text{H}(1\text{D}) \cdots \text{Cl}(2)$ 170(3)°]; furthermore, hydrogen bonds

Table 1 Selected bond lengths (Å) and angles (°) for [NiL(H₂O)](ClO₄)₂·H₂O **4**, [NiL(Cl)]Cl·H₂O **5**, [NiL(SCN)]BF₄ **6**, [NiL(eseu)](BF₄)₂ **7** and [NiL(py)](BF₄)₂ **8**^a

	4	5	6	7	8
Ni–N(1)	2.019(7)	2.033(2)	2.037(3)	2.020(6)	2.007(12)
Ni–N(2)	2.022(7)	2.041(2)	2.037(3)	2.023(5)	2.005(12)
Ni–S(1)	2.439(3)	2.4545(11)	2.4456(10)	2.428(2)	2.417(5)
Ni–S(2)	2.462(3)	2.4761(11)	2.4701(10)	2.481(2)	2.385(4)
Ni–S(3)	2.404(3)	2.4445(10)	2.4212(10)	2.440(2)	2.403(5)
Ni–X	2.089(6)	2.3693(10)	2.012(3)	2.5927(12)	2.057(12)
S(1)–Ni–N(1)	81.8(2)	81.49(6)	81.42(8)	81.6(2)	82.7(4)
S(1)–Ni–N(2)	162.6(2)	161.93(7)	161.69(8)	162.7(2)	160.5(4)
S(1)–Ni–X	87.8(2)	88.53(3)	91.19(9)	89.16(5)	89.4(4)
S(1)–Ni–S(2)	115.89(9)	116.64(3)	118.02(4)	115.72(7)	114.6(2)
S(2)–Ni–N(1)	162.1(2)	161.74(5)	158.94(8)	162.3(2)	162.6(3)
S(2)–Ni–N(2)	81.5(2)	81.10(7)	80.28(8)	81.1(2)	83.5(4)
S(2)–Ni–S(3)	86.05(8)	85.43(3)	85.51(3)	85.78(6)	85.9(2)
S(3)–Ni–S(1)	88.00(9)	85.20(7)	87.33(3)	85.30(6)	87.0(2)
S(3)–Ni–N(1)	91.9(2)	94.49(7)	87.56(7)	92.4(2)	93.2(3)
S(3)–Ni–N(2)	92.9(2)	93.25(7)	94.13(8)	92.19(14)	87.1(3)
S(3)–Ni–X	172.5(2)	169.47(3)	170.73(9)	172.43(6)	172.9(4)
N(1)–Ni–N(2)	80.8(3)	80.68(8)	80.41(11)	81.4(2)	79.1(5)
N(1)–Ni–X	93.7(3)	92.94(7)	101.28(11)	91.86(14)	92.4(5)
N(2)–Ni–X	93.0(3)	95.31(7)	90.15(11)	94.62(14)	98.2(5)
S(2)–Ni–X	90.2(2)	89.85(3)	87.12(8)	92.00(5)	90.0(3)

^a X = O (H₂O), Cl, N (SCN), Se (eseu) and N (py) for complexes **4**, **5**, **6**, **7** and **8** respectively; the same numbering scheme has been adopted for all the five complexes (see Fig. 1).

between the unco-ordinated Cl[−] ions and the H(1A) and H(1B) hydrogens of two CH₂ groups next to the phenanthroline moieties [H(1B)⋯Cl(2) 2.68, H(1A)⋯Cl(2ⁱ) 2.66 Å, *i* 3 − *x*, 1 − *y*, 1 − *z*] generate dimeric units of the complex cation (Fig. 2). In complex **6** the SCN[−] ion binds the Ni^{II} through its nitrogen atom [Ni–N(3) 2.012(3) Å, Ni–N(3)–C(19) 157.3(3), S(3)–Ni–N(3) 170.73(9)°] instead of through the softer sulfur donor (Table 1). In complex **7** the co-ordinated imidazoline ring [Ni–Se 2.5927(12) Å, Ni–Se–C(1L) 103.80(2), S(3)–Ni–Se 172.43(6)°] is almost parallel to the phenanthroline moiety of the macrocycle with an interannular interaction between the imidazoline ring and the phenanthroline moiety of 3.636(6) Å (Fig. 3). The complex cations interact in a pairwise fashion and the structure is determined by secondary interactions between the selenium atom of one complex cation and the two sulfur atoms in the basal co-ordination plane from the other [Se⋯S(1ⁱ) 3.485(2) and Se⋯S(2ⁱ) 3.512(2) Å, *i* −*x*, 1 − *y*, 1 − *z*]. The S⋯S interactions between the two co-ordinated L molecules [3.505(2) Å] and very weak Se⋯H contacts (3.053 Å) contribute to the association of the two complex cations, imposing a cubane-like arrangement on the Ni₂Se₂S₄ core framework (Fig. 3). Finally, the structure of [NiL(py)](BF₄)₂ **8** also confirms six co-ordination at Ni^{II} with L adopting a square-based pyramidal geometry at the metal and the pyridine molecule axially co-ordinated to complete a distorted octahedral co-ordination sphere [Ni–N(3) 2.057(12) Å, S(3)–Ni–N(3) 172.9(4)°] (Table 1). The reaction of [NiL(MeCN)](BF₄)₂ **1** with the ligands Br[−], CN[−], aniline or etu affords microcrystalline products after crystallization from MeCN–Et₂O (see Experimental section); analytical data, IR and FAB mass spectroscopy suggest the formulation [NiL(L′)]BF₄ (**9**, **10**) and [NiL(L′)](BF₄)₂ (**11**, **12**) for all of these but unfortunately no single crystal suitable for X-ray diffraction studies has been obtained.

The substitution reactions of the co-ordinated acetonitrile molecule in complex **1** has been followed by UV-visible spectrophotometric titrations, carried out in MeCN solution, using anionic and neutral ligands L′ [Cl[−], Br[−], I[−], CN[−], SCN[−], H₂O, pyridine, aniline, 1,3-dimethyl-4-imidazoline-2-thione or 1,3-dimethyl-4-imidazoline-2-selone]. The presence of at least one isosbestic point (see Fig. 4) indicates that only two absorbing species are involved in the reaction, according to equilibrium (1) where (2 − *n*) equals 1 or 2 depending on the charge (−1

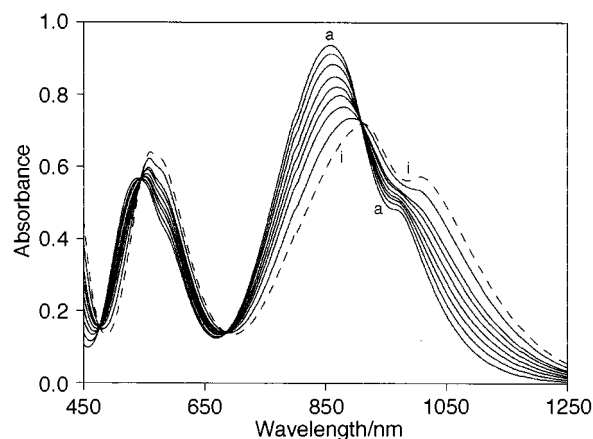
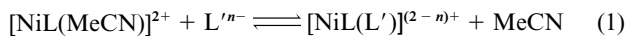


Fig. 4 The UV-visible spectra of mixtures of [NiL(MeCN)](BF₄)₂ **1** and Et₄NCl, showing four isosbestic points at 476, 554, 685 and 910 nm. [1] = 1.56 × 10^{−2} mol dm^{−3} and [Et₄NCl] = 0, 1.56 × 10^{−3}, 3.12 × 10^{−3}, 4.68 × 10^{−3}, 6.24 × 10^{−3}, 7.80 × 10^{−3}, 9.36 × 10^{−3}, 1.25 × 10^{−2} and 1.56 × 10^{−2} mol dm^{−3} for (a), (b), (c), (d), (e), (f), (g), (h) and (i) respectively. For clarity only the first and the last of these spectra have been labelled.



or 0) of the titrant ligand L′. The presence of only two species involved in the equilibrium has also been confirmed by a factor analysis¹¹ of the electronic spectra recorded after each addition of L′. In all the titrations with the anionic ligands the initial spectrum changes with increasing amounts of L′ added until the 1 : 1 [L′]:[1] molar ratio is reached. On addition of an excess of L′ the spectrum does not change further, indicating that the substitution reaction is quantitative. The dashed line in Fig. 4 has been recorded for the 1 : 1 [Cl[−]]:[1] molar ratio and corresponds to the spectrum of a pure sample of [NiL(Cl)]⁺ at the same concentration. Analogous behaviour has been observed for all the other anionic ligands. The quantitative nature of these titrations[‡] is also confirmed by the plots of the absorb-

[‡] Reactions of complex **1** with anionic ligands may have an equilibrium nature but the corresponding equilibrium constants should be very high; consequently, their spectrophotometric determination cannot give reliable values.

Table 2 Equilibrium constants ($\text{dm}^3 \text{mol}^{-1}$; MeCN; $T = 25^\circ\text{C}$) for the substitution reaction of MeCN in $[\text{NiL}(\text{MeCN})][\text{BF}_4]_2$ **1** with the neutral ligands (L'). Standard deviations in parentheses

L'	K_{eq}^a	s^b	K_{eq}^c
H_2O	70(5)	0.31–0.77	139(29)
etu	16(1)	0.14–0.64	32(3)
eseu	39(2)	0.30–0.85	32(3)
py	306(16)	0.62–0.98	123(30)
an	9(2)	0.09–0.73	13(0.3)

^a Calculated from a non-linear least-squares method.¹² ^b Saturation fraction defined as the ratio between the concentration of the complex formed and the analytical concentration of **1**. ^c Calculated from distribution curves.

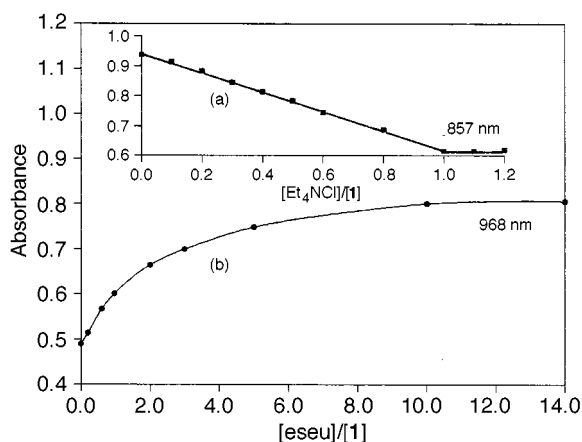


Fig. 5 Plots of the absorbance values versus the $[L']:[1]$ molar ratios at different wavelengths for the titrations of $[\text{NiL}(\text{MeCN})][\text{BF}_4]_2$ **1** with Et_4NCl (a) and eseu (b).

ance values versus the $[L']:[1]$ molar ratios, which always show two straight lines crossing at the $[L']:[1]$ value of 1:1 [Fig. 5(a) for the case of Cl^-]. In the titrations with the neutral ligands (H_2O , py, an, etu or eseu) the spectra continue to exhibit changes even when the $[L']:[1]$ molar ratio exceeds 1:1 [see Fig. 5(b) for the case of $L' = \text{eseu}$]. In these cases, from the distribution curves, it has been possible to make a preliminary estimate of the equilibrium constants of reaction (1) for all five neutral ligands and the values obtained have been deposited as SUP 57496. However, in order to obtain more reliable K_{eq} values, especially for the cases in which the spectral features of the two absorbing species **1** and $[\text{NiL}(L')]^{2+}$ are very similar ($L' = \text{py}$, etu or H_2O), we have also calculated them by using a non-linear least-squares program¹² on the same set of spectra from which the distribution curves were computed. The obtained K_{eq} values (Table 2) show that the best donor is pyridine, followed by water, whereas eseu is a better donor than its sulfur analogue etu.

The redox properties of complex **1**, monitored by cyclic voltammetry in MeCN solution ($0.1 \text{ mol dm}^{-3} \text{ Bu}^n\text{NBF}_4$) have been previously described.⁹ A quasi-reversible reduction at ${}^1E_{\text{pc}} = -0.98 \text{ V}$ vs. ferrocene–ferrocenium, assigned to a metal-based $\text{Ni}^{\text{II}}-\text{Ni}^{\text{I}}$ couple, and a second broad irreversible process at ${}^2E_{\text{pc}} = -1.91 \text{ V}$, presumably due to the $\text{Ni}^{\text{I}}-\text{Ni}^{\text{0}}$ couple, were observed. Coulometric measurements in MeCN under argon at controlled potential show the first reduction to be a one-electron process with formation of a brown precipitate. This precipitate, obtained by electrolytic process on the first reduction peak carried out at room temperature and at -20°C , was diamagnetic and ESR silent at 77 K and gave satisfactory elemental analysis for $[\text{NiL}]\text{BF}_4$. This might indicate the formation of a binuclear complex having a $\text{Ni}^{\text{I}}-\text{Ni}^{\text{0}}$ bond, as reported for some nickel(II) complexes with tetraazamacrocyclic ligands.¹³ The cyclic voltammetry of **1** has also been recorded in MeCN under an atmosphere of carbon monoxide (Fig. 6) with the aim of isolating the paramagnetic nickel(II) complex before

Table 3 Reduction peaks versus Fc/Fc^+ obtained by cyclic voltammetry in dmf solution for all the nickel(II) complexes synthesized (supporting electrolyte $0.1 \text{ mol dm}^{-3} \text{ Bu}^n\text{NBF}_4$, scan rate 100 mV s^{-1})

Complex	${}^1E_{\text{pc}}/\text{V}$	${}^2E_{\text{pc}}^a/\text{V}$
1 $[\text{NiL}(\text{MeCN})][\text{BF}_4]_2^b$	-1.23 ^c	-1.96
2 $[\text{NiL}(\text{Cl})]\text{BF}_4^d$	-1.42	-1.95
9 $[\text{NiL}(\text{Br})]\text{BF}_4$	-1.35	-1.95
3 $[\text{NiL}(\text{I})]\text{I}_3$	-1.18	-1.99
10 $[\text{NiL}(\text{CN})]\text{BF}_4$	-1.36	-1.98
6 $[\text{NiL}(\text{SCN})]\text{BF}_4$	-1.48	-2.03
7 $[\text{NiL}(\text{eseu})][\text{BF}_4]_2^b$	-1.15 ^c	-1.94
12 $[\text{NiL}(\text{etu})][\text{BF}_4]_2^b$	-1.12 ^c	-1.92
8 $[\text{NiL}(\text{py})][\text{BF}_4]_2^b$	-1.14 ^c	-1.92
11 $[\text{NiL}(\text{an})][\text{BF}_4]_2^b$	-1.11 ^c	-1.92

^a The second reduction process is irreversible for all complexes. ^b As shown by electronic spectroscopy, this complex undergoes a partial substitution of the co-ordinated L' with a solvent molecule in dmf. ^c The reduction process is quasi-reversible and becomes reversible [$i_p(\text{anodic}) = i_p(\text{cathodic})$, $\Delta E = 0.056 \text{ mV}$] at low potential scan speed; ΔE ranges from 0.14 to 0.20 V at 100 mV s^{-1} . ^d The reduction peaks of $[\text{NiLCl}]\text{Cl}\cdot\text{H}_2\text{O}$ **5** are the same as those of **2**.

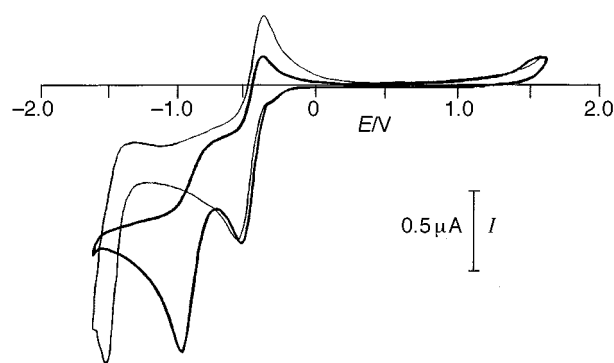


Fig. 6 Cyclic voltammograms in MeCN of complex **1** in an atmosphere of argon (thin line) and CO (thick line). Scan rate 100 mV s^{-1} , supporting electrolyte $0.1 \text{ mol dm}^{-3} \text{ Bu}^n\text{NBF}_4$.

it can dimerize. The shift of the second reduction process from ca. -1.5 (vs. $\text{Ag}-\text{AgCl}$) to ca. -1.0 V indicates an interaction of the species from this reduction process with CO, but again no ESR signal has been detected at 77 K from the brown precipitate obtained after coulometry at the first reduction potential. The same results were obtained by carrying out the cyclic voltammetry and the reductive controlled-potential electrolysis upon the first reduction process under the same condition as before but in the presence of $\text{P}(\text{OMe})_3$, and under argon. The cyclic voltammogram for complex **1** was then measured under argon in MeCN in the presence of PME_3 and a very small shift was observed for the primary reduction wave to more negative potential. After reductive controlled-potential electrolysis at room temperature on the first reduction peak a pale green solution was obtained which showed an isotropic ESR spectrum as a frozen glass (77 K) with a g_{iso} value of 2.12 assigned to the $[\text{Ni}^{\text{I}}\text{L}(\text{PME}_3)]^+$ species. This clearly indicates that the first reduction wave in the cyclic voltammogram of **1** is metal based and corresponds to the initial formation of the $[\text{Ni}^{\text{I}}\text{L}]^+$ species rather than to the formation of a nickel(II) ligand radical species $[\text{Ni}^{\text{II}}(\text{L}^{\cdot-})]^+$.¹⁴ The cyclic voltammetry (CV) measurements (Table 3) on all the complexes obtained from **1** by substituting the MeCN molecule with anionic ligands have been carried out in dmf solutions for solubility reasons. The first reduction wave is completely irreversible for $L' = \text{Cl}^-$, Br^- , I^- , CN^- or SCN^- ; the substantial variation of the ${}^1E_{\text{pc}}$ value on changing the nature of the anionic ligand L' (Table 3) is further evidence of the reduction process being metal based (i.e. $\text{Ni}^{\text{II}} \rightarrow \text{Ni}^{\text{I}}$). Cyclic voltammetry was also carried out in dmf in the case of $[\text{NiL}(L')]^{2+}$ complexes obtained with neutral ligands and it shows the first reduction process to be

quasi-reversible and to have a narrow range of variability for E_{pc} between -1.11 and -1.23 V (vs. Fc/Fc⁺; Table 3). This is probably due to the presence of the equilibrium (1) which occurs in MeCN as well as in dmf solution as shown by spectrophotometric measurements. A second irreversible reduction process is present for all the studied complexes (Table 3).

In conclusion, the present study clearly confirms the ability of L to encapsulate Ni^{II}, blocking five of the co-ordination sites around the metal, leaving the sixth free to be occupied by various other ligands. This represents an ideal case for studying thermodynamically competitive substitution reactions at the metal, whereas from a synthetic point of view it offers the possibility of using the [NiL]²⁺ cation as a building block for the design of more complex systems, for example multi-centred compounds with multidentate ligands.

Experimental

All melting points are uncorrected. Microanalytical data were obtained on a Fisons EA 1108 CHNS-O instrument operating at 1000 °C. The IR spectra (4000–400 cm⁻¹) were recorded as KBr pellets using a Perkin-Elmer 983 spectrophotometer and a 7500 Data Station.

The UV-visible measurements were carried out in MeCN solution by using a Varian Cary 5 UV-Vis-NIR spectrophotometer equipped with a temperature controller accessory and connected to an IBM PS/2 computer. The spectra of several solutions were recorded in the range 450–1250 nm at 25 °C, keeping the concentration of complex **1** constant and varying that of L' up to a [L']:[**1**] molar ratio of *ca.* 1.2:1 for anionic (beyond this limit a solid starts precipitating) and *ca.* 15:1 for neutral ligands L'. The spectra recorded for each ligand L' were analysed using the program SPECFIT¹¹ to determine the number of species present in solution. In all cases the presence of only two species was confirmed. Subsequently, the spectra were deconvoluted into their constituent Gaussian peaks.¹⁵ From the heights of these peaks, the molar absorption coefficients for the two species in equilibrium were evaluated and the distribution curves computed.¹⁵ In the case of the reactions with the neutral ligands, the same set of spectra were also used to calculate the K_{eq} values by a program based on a non-linear least-squares method.¹² This program assumes that the best values of K_{eq} and ϵ are those which minimize the sum of the function $\chi^2 = \sum(A_c - A_s)^2/(N - 2)$, where A_c and A_s are the calculated and experimental absorbances and N is the number of data points. The optimization of K_{eq} values was carried out using four different wavelengths. In the Preparation section (see below), the UV-visible spectra reported for complexes **4**, **7**, **8**, **11** and **12** are those recorded at the end of the spectrophotometric titration of **1** with the appropriate neutral ligand; for **5**, **6**, **9** and **10** they refer to MeCN solutions of **1** and the appropriate anionic ligand in 1:1 molar ratio.

Cyclic voltammetry was performed using a conventional three-electrode cell, with a platinum double-bead electrode and Ag–AgCl reference electrode. All measurements were taken under an argon atmosphere in a 0.1 mol dm⁻³ solution of Bu₄NBF₄ in dmf or MeCN, which were freshly distilled from MgSO₄ and CaH₂ respectively, prior to use. Scan rates ranged from 50 to 400 mV s⁻¹. Data were recorded on a computer controlled Model 273 EG & G (Princeton Applied Research) potentiostat galvanostat using Model 270 electrochemical analysis software. The ESR spectra were recorded by using a Bruker ER-200D spectrometer.

The isosbestic points in the spectrophotometric titration of complex **1** with L', and the K_{eq} values estimated from the distribution curves have been deposited as SUP 57496.

Preparations

The macrocyclic ligand L and the complexes **1–3** were synthesized according to the procedure previously reported.⁹

[NiL(H₂O)](ClO₄)₂·H₂O **4.** A solution of Ni(ClO₄)₂·6H₂O (128 mg, 0.35 mmol) in MeCN (1.5 cm³) was added to a solution of L (128 mg, 0.35 mmol) in CH₂Cl₂ (1.5 cm³). The violet microcrystalline solid which formed was filtered off and recrystallized from methanol (130 mg, 58% yield), mp 141 °C with decomposition [Found (Calc. for C₁₈H₂₂Cl₂N₂NiO₁₀S₃): C, 32.8 (33.2); H, 3.6 (3.4); N, 4.1 (4.3); S, 15.7 (14.8)%]. Electronic spectrum in MeCN: 553 (30), 873 (60) and 967 nm (55 dm³ mol⁻¹ cm⁻¹); 10Dq = 11460 cm⁻¹. IR (KBr pellet), $\tilde{\nu}/\text{cm}^{-1}$: 3407m, 3059w, 2964w, 2921w, 1621m, 1590m, 1576m, 1499m, 1415m, 1391m, 1275w, 1088s, 923w, 885m, 853m, 733m, 636m, 625s and 542w.

[NiL(Cl)]Cl·H₂O **5.** A solution of NiCl₂·6H₂O (88 mg, 0.35 mmol) in CH₂Cl₂ (1.5 cm³) was added to a solution of L (128 mg, 0.35 mmol) in CH₂Cl₂ (1.5 cm³). A pale green microcrystalline solid was formed, which was filtered off and recrystallized from *n*-butanol (154 mg, 88% yield), mp 241 °C with decomposition [Found (Calc. for C₁₈H₂₀Cl₂N₂NiOS₃): C, 42.5 (42.7); H, 4.1 (4.0); N, 5.1 (5.5); S, 18.4 (19.0)%]. Electronic spectrum in MeCN: 560 (41), 579 (shoulder) (40), 912 (46) and 1011 nm (35 dm³ mol⁻¹ cm⁻¹); 10Dq = 10960 cm⁻¹. IR (KBr pellet), $\tilde{\nu}/\text{cm}^{-1}$: 3383s, 3079w, 2967w, 1621m, 1589m, 1486m, 1419m, 1386m, 1179w, 923w, 887m, 859m, 723w and 537w.

[NiL(SCN)]BF₄·MeNO₂ **6.** Addition of Bu₄N⁺SCN⁻ (14.3 mg, 0.047 mmol) to a solution of complex **1** (30 mg, 0.047 mmol) in MeCN followed by crystallization from MeNO₂–Et₂O afforded purple blocky crystals of **6** (16.5 mg, 62% yield), mp 240 °C with decomposition [Found (Calc. for C₂₀H₂₁BF₄N₄NiO₂S₄): C, 38.2 (38.5); H, 3.4 (3.4); N, 8.9 (9.0); S, 20.5 (20.6)%]. FAB mass spectrum (3-nitrobenzyl alcohol matrix): *m/z* 474, 416; calc. for [⁵⁸NiL(SCN)]⁺ and [⁵⁸NiL]⁺ *m/z* 474 and 416 respectively. Electronic spectrum in MeCN: 552 (53), 889 (67) and 975 nm (53 dm³ mol⁻¹ cm⁻¹); 10 Dq = 11250 cm⁻¹. IR (KBr pellet), $\tilde{\nu}/\text{cm}^{-1}$: 3080w, 2910w, 2077s, 1590m, 1574m, 1485m, 1429m, 1395m, 1372m, 1061s, 886m, 855m and 522w.

[NiL(eseu)](BF₄)₂ **7.** 1,3-Dimethyl-4-imidazoline-2-selone (0.28 g, 1.58 mmol) was added to a solution of complex **1** (50 mg, 0.079 mmol) in MeCN. Crystallization from MeCN–Et₂O afforded dark red blocky crystals of **7** (40 mg, 67% yield), mp 255 °C with decomposition [Found (Calc. for C₂₃H₂₆B₂F₈N₄NiS₃Se): C, 36.1 (35.9); H, 3.6 (3.4); N, 7.4 (7.3); S, 12.4 (12.5)%]. FAB mass spectrum (3-nitrobenzyl alcohol matrix): *m/z* 416; calc. for [⁵⁸NiL]⁺ *m/z* 416. Electronic spectrum in MeCN: 890 (59) and 1058 nm (shoulder) (19 dm³ mol⁻¹ cm⁻¹); 10 Dq = 11240 cm⁻¹. IR (KBr pellet), $\tilde{\nu}/\text{cm}^{-1}$: 3190w, 3170w, 3109w, 2925w, 1590w, 1572w, 1485m, 1422m, 1383m, 1238w, 1060s, 884m, 857m, 740w, 722w, 534w and 522w.

[NiL(py)](BF₄)₂ **8.** Pyridine (2.6 cm³ of 0.6 mol dm⁻³ solution in MeCN, 1.58 mmol) was added to a solution of complex **1** (50 mg, 0.079 mmol) in MeCN. Crystallization from MeCN–Et₂O afforded purple columnar crystals of **8** (38 mg, 72% yield), mp 241 °C with decomposition [Found (Calc. for C₂₃H₂₃B₂F₈N₃NiS₃): C, 41.4 (41.2); H, 3.6 (3.5); N, 6.3 (6.3); S, 14.4 (14.4)%]. FAB mass spectrum (3-nitrobenzyl alcohol matrix): *m/z* 416; calc. for [⁵⁸NiL]⁺ *m/z* 416. Electronic spectrum in MeCN: 538 (55), 873 (65) and 979 nm (shoulder) (36 dm³ mol⁻¹ cm⁻¹); 10 Dq = 11460 cm⁻¹. IR (KBr pellet), $\tilde{\nu}/\text{cm}^{-1}$: 3077w, 2985w, 2956w, 2921w, 1606m, 1588m, 1488m, 1445m, 1439m, 1422m, 1290w, 1049s, 895m, 863m, 796m, 727m, 638w, 521m and 432w.

[NiL(Br)]BF₄ **9.** Addition of Bu₄NBr (25.5 mg, 0.079 mmol) to a solution of complex **1** (50 mg, 0.079 mmol) in MeCN, followed by crystallization from MeCN–Et₂O, afforded green microcrystals of **9** (30 mg, 65% yield), mp 235 °C with decomposition [Found (Calc. for C₁₈H₁₈BBF₄N₂NiS₃): C, 37.1

Table 4 Summary of crystal data

Compound	[NiL(H ₂ O)]ClO ₄ ·H ₂ O 4	[NiL(Cl)]Cl·H ₂ O 5	[NiL(SCN)]BF ₄ ·MeNO ₂ 6	[NiL(eseu)]BF ₄ 7	[NiL(py)]BF ₄ 8
Formula	C ₁₈ H ₂₂ Cl ₂ N ₂ NiO ₁₀ S ₃	C ₁₈ H ₂₀ Cl ₂ N ₂ NiO ₈ S ₃	C ₂₀ H ₁₇ BF ₄ N ₄ NiO ₂ S ₄	C ₃₃ H ₃₆ B ₃ F ₈ N ₃ NiS ₃ Se	C ₃₃ H ₃₆ B ₃ F ₈ N ₃ NiS ₃
<i>M</i>	652.17	506.15	623.17	765.95	669.95
Crystal appearance	Purple plate	Green prism	Purple block	Red block	Purple column
Crystal size/mm	0.34 × 0.30 × 0.20	0.36 × 0.34 × 0.22	0.24 × 0.20 × 0.18	0.22 × 0.18 × 0.14	0.62 × 0.29 × 0.19
Crystal system	Orthorhombic	Triclinic	Monoclinic	Triclinic	Monoclinic
Space group	<i>Pbca</i> (no. 61)	<i>P</i> $\bar{1}$ (no. 2)	<i>P</i> 2 ₁ / <i>c</i> (no. 14)	<i>P</i> $\bar{1}$ (no. 2)	<i>P</i> 2 ₁ / <i>n</i> (no. 14)
<i>a</i> /Å	15.830(2)	10.972(3)	15.606(2)	11.260(1)	10.27(2)
<i>b</i> /Å	22.432(2)	11.472(2)	12.292(1)	11.678(2)	13.50(2)
<i>c</i> /Å	14.249(2)	10.264(2)	13.671(2)	12.049(1)	18.27(2)
<i>a</i> °	—	99.23(1)	—	77.607(11)	—
<i>β</i> °	—	117.28(1)	110.749(13)	68.151(9)	—
<i>γ</i> °	—	109.41(1)	—	77.320(11)	—
<i>U</i> /Å ³	5059.8(9)	1004.9(4)	2452.4(5)	1419.2(3)	2533(7)
<i>Z</i>	8	2	4	2	4
<i>T</i> /K	294(2)	294(2)	150(2)	150(2)	220(2)
<i>μ</i> (Mo-Kα)/mm ⁻¹	1.282	1.555	1.19	2.263	1.094
Diffractometer	Rigaku AFC5S	Rigaku AFC5S	Enraf-Nonius FAST	Siemens P4	Stoe Stadi-4
Reflections collected	4459	3543	9967	6363	4986
Unique reflections, <i>R</i> _{int}	4459, —	3543, —	3751, 0.067	4078, 0.078	4590, 0.038
<i>R</i> 1	0.0657 [2302 <i>I</i> ≥ 2σ(<i>I</i>)]	0.0442 [2707 <i>I</i> ≥ 2σ(<i>I</i>)]	0.0338 [2730 <i>I</i> ≥ 2σ(<i>I</i>)]	0.0446 [2507 <i>I</i> ≥ 2σ(<i>I</i>)]	0.1143 [3762 <i>I</i> ≥ 2σ(<i>I</i>)]
<i>wR</i> 2 (all data)	0.169	0.128	0.0715	0.107	0.363

(37.0); H, 3.2 (3.1); N, 4.9 (4.8); S, 16.4 (16.5)%]. FAB mass spectrum (3-nitrobenzyl alcohol matrix): m/z 497, 416; calc. for $^{58}\text{NiL}(\text{Br})^+$ and $^{58}\text{NiL}^+$ m/z 496 and 416 respectively. Electronic spectrum in MeCN: 564 (48), 922 (48) and 1025 nm (33 $\text{dm}^3 \text{mol}^{-1} \text{cm}^{-1}$); 10 $Dq = 10850 \text{cm}^{-1}$. IR (KBr pellet), $\tilde{\nu}/\text{cm}^{-1}$: 3080w, 2976w, 2886w, 1590m, 1574m, 1500m, 1486m, 1392m, 1373m, 1061s, 935m, 886m, 852s, 726m, 685m, 542m and 521m.

[NiL(CN)]BF₄ 10. Addition of Bu^n_4NCN (12.8 mg, 0.047 mmol) to a solution of complex **1** (30 mg, 0.047 mmol) in MeCN, followed by crystallization from MeCN–Et₂O, afforded pink microcrystals of **10** (15 mg, 60% yield), mp 230 °C with decomposition [Found (Calc. for C₁₉H₁₈BF₄N₃NiS₃): C, 43.0 (43.1); H, 3.3 (3.4); N, 7.8 (7.9); S, 18.2 (18.1)%]. FAB mass spectrum (3-nitrobenzyl alcohol matrix): m/z 442, 416; calc. for $^{58}\text{NiL}(\text{CN})^+$ and $^{58}\text{NiL}^+$ m/z 442 and 416 respectively. Electronic spectrum in MeCN: 529 (44), 872 (45) and 975 nm (shoulder) (30 $\text{dm}^3 \text{mol}^{-1} \text{cm}^{-1}$); 10 $Dq = 11470 \text{cm}^{-1}$. IR (KBr pellet), $\tilde{\nu}/\text{cm}^{-1}$: 3070w, 2917w, 2143m, 1620m, 1486m, 1432m, 1422m, 1057s, 939m, 886m, 522w and 428w.

[NiL(an)]BF₄ 11. Aniline (2.6 cm^3 of solution 0.6 mol dm^{-3} in MeCN, 1.58 mmol) was added to a solution of complex **1** (50 mg, 0.079 mmol) in MeCN. Crystallization from MeCN–Et₂O afforded dark pink microcrystals of **11** (30 mg, 56% yield), mp 238–239 °C with decomposition [Found (Calc. for C₂₄H₂₅B₂F₈N₃NiS₃): C, 42.3 (42.2); H, 3.5 (3.4); N, 6.3 (6.2); S, 13.9 (14.1)%]. FAB mass spectrum (3-nitrobenzyl alcohol matrix): m/z 433, 416; calc. for $^{58}\text{NiL}(\text{NH}_2)^+$ and $^{58}\text{NiL}^+$ m/z 433 and 416 respectively. Electronic spectrum in MeCN: 542 (46), 877 (61) and 997 nm (shoulder) (33 $\text{dm}^3 \text{mol}^{-1} \text{cm}^{-1}$); 10 $Dq = 11400 \text{cm}^{-1}$. IR (KBr pellet), $\tilde{\nu}/\text{cm}^{-1}$: 3319m, 3278m, 3180w, 3075w, 3039w, 2987w, 2928w, 1593s, 1491s, 1415m, 1396m, 1261w, 1047s, 886m, 856m, 802m, 763m, 701m and 522m.

[NiL(etu)]BF₄ 12. 1,3-Dimethyl-4-imidazoline-2-thione (etu) (0.2 g, 1.58 mmol) was added to a solution of complex **1** (50 mg, 0.079 mmol) in MeCN. Crystallization from MeCN–Et₂O afforded dark green microcrystals of **12** (30 mg, 53% yield), mp 242–243 °C with decomposition [Found (Calc. for C₂₃H₂₆B₂F₈N₄NiS₄): C, 38.6 (38.4); H, 3.8 (3.9); N, 7.8 (7.8); S, 17.8 (17.8)%]. FAB mass spectrum (3-nitrobenzyl alcohol matrix): m/z 416; calc. for $^{58}\text{NiL}^+$ m/z 416. Electronic spectrum in MeCN: 547 (62), 879 (61) and 1054 nm (shoulder) (23 $\text{dm}^3 \text{mol}^{-1} \text{cm}^{-1}$); 10 $Dq = 11380 \text{cm}^{-1}$. IR (KBr pellet), $\tilde{\nu}/\text{cm}^{-1}$: 3175w, 3145w, 3121w, 2937w, 2334w, 1591m, 1572m, 1484m, 1431m, 1422m, 1390m, 1240m, 1057s, 884m, 858m, 750w, 733w, 723w, 675w, 535w and 521m.

Crystallography

Crystal data for all five structure determinations appear in Table 4. Only special features of the analyses are noted here.

[NiL(H₂O)]ClO₄·H₂O 4 and [NiL(Cl)]Cl·H₂O 5. Single-crystal data collections were performed using ω – 2θ scans. Both datasets were corrected for Lorentz-polarization effects, and for absorption by means of ψ scans (transmission factor ranges were 0.909–1.00 for **4** and 0.842–1.00 for **5**). The structures were solved by direct methods using SHELXS 86¹⁶ and full-matrix least-squares refinements on F^2 were performed using SHELXL 93.¹⁷ Non-hydrogen atoms of **4** were refined with anisotropic displacement parameters and hydrogen atoms were introduced at geometrically calculated positions and thereafter allowed to ride on their parent atoms. The structure of **5** shows disorder of the carbon atoms C(16) and C(17), each component of which is approximately half occupied. Partially occupied hydrogen atoms were not included, but other hydrogen atoms were treated as for **4** and non-hydrogen atoms were refined with anisotropic displacement parameters.

[NiL(SCN)]BF₄·MeNO₂ 6. The crystal was cooled to 150 K using an Oxford Cryosystem open flow cryostat¹⁸ and data were acquired using area detector scans.¹⁹ The structure was solved by a combination of direct and Fourier methods using SHELXS 96¹⁶ and full-matrix least-squares refinements on F^2 were performed using SHELXL 96.¹⁷ All non-H atoms were refined anisotropically and H atoms were placed in calculated positions and thereafter allowed to ride on their parent atoms.

[NiL(eseu)]BF₄ 7. The crystal was cooled to 150 K using an Oxford Cryosystem open-flow nitrogen cryostat.¹⁸ Data were acquired as ω scans. The structure was solved by direct methods using SHELXS 97¹⁶ and full-matrix least-squares refinements on F^2 were performed using SHELXL 97.¹⁷ All non-H atoms were refined anisotropically and H atoms were placed geometrically and thereafter allowed to ride on their parent atoms. Disorder in the BF₄[–] anions was identified and modelled. For one anion two independent orientations could be identified. Similarity restraints¹⁷ were applied to B–F and F···F distances. The F atoms of the major (0.76) component were refined anisotropically, those of the minor (0.24) isotropically. In the second anion it was only possible to identify two components for one F atom: these were refined as above and the final occupancies were 0.84 and 0.16 for major and minor components, respectively.

[NiL(py)]BF₄ 8. The crystal was cooled to 220 K using an Oxford Cryosystem open-flow nitrogen cryostat¹⁸ and data were acquired as ω – θ scans using on-line profile fitting.²⁰ Numerical corrections (transmission factor ranges were 0.764–0.839) for the effects of absorption were applied and the structure was solved by direct methods¹⁶ and refined¹⁷ with anisotropic displacement parameters for all fully occupied non-H atoms. Pseudo-orthorhombic twinning was detected and successfully included in the model using the twin law (100/0–10/00–1): twin components were found to occur in the ratio 0.78:0.22. The largest features in the final ΔF synthesis lie within 1.1 Å of the Ni atom.

CCDC reference number 186/1338.

See <http://www.rsc.org/suppdata/dt/1999/1085/> for crystallographic files in .cif format.

Acknowledgements

We thank the Comitato Nazionale per le Scienze Chimiche of Consiglio Nazionale delle Ricerche of Rome and the EPSRC and University of Nottingham (UK) for the financial support. L. E., V. M. and J. C. acknowledge the financial support of Comisión Interministerial de Ciencia i Tecnologia (C.I.C.Y.T.) of the Spanish Government provided by the project MAT97-0720. Support from the Academy of Finland is acknowledged by R. K. and R. S. We also thank the EPSRC National Service for Mass Spectrometry at Swansea.

References

- 1 K. Wieghardt and P. Chaudhuri, *Prog. Inorg. Chem.*, 1987, **35**, 329; S. R. Cooper, *Acc. Chem. Res.*, 1988, **21**, 141; A. J. Blake and M. Schröder, *Adv. Inorg. Chem.*, 1990, **35**, 1; C. E. Housecroft, *Coord. Chem. Rev.*, 1992, **115**, 141; G. Reid and M. Schröder, *Chem. Soc. Rev.*, 1990, **19**, 239.
- 2 A. McAuley, P. R. Norman and O. Olubuyiale, *Inorg. Chem.*, 1984, **23**, 1938; S. Chandrasekhar and A. McAuley, *Inorg. Chem.*, 1992, **31**, 2234 and refs. therein; A. J. Blake, M. A. Halcrow and M. Schröder, *J. Chem. Soc., Dalton Trans.*, 1992, 2803; A. J. Blake, G. Reid and M. Schröder, *J. Chem. Soc., Dalton Trans.*, 1994, 329 and refs. therein; G. J. Grant, K. E. Rogers, W. N. Setzer and D. G. Van Derveer, *Inorg. Chim. Acta*, 1995, **234**, 35; C. Landgrafe and W. S. Sheldrick, *J. Chem. Soc., Dalton Trans.*, 1996, 989; M. P. Suh, K. Y. Oh, J. W. Lee and Y. Y. Boe, *J. Am. Chem. Soc.*, 1996, **118**, 777 and refs. therein.
- 3 V. McKee, *Adv. Inorg. Chem.*, 1993, **40**, 323.

- 4 M. M. Bishop, J. Lewis, D. O'Donoghue and P. R. Raithby, *J. Chem. Soc., Chem. Commun.*, 1978, 476; C. W. G. Ansell, J. Lewis, M. C. Liptrot, P. R. Raithby and M. Schröder, *J. Chem. Soc., Dalton Trans.*, 1982, 1593; C. W. G. Ansell, J. Lewis, P. R. Raithby, J. N. Ramsden and M. Schröder, *J. Chem. Soc., Chem. Commun.*, 1982, 546; D. Parker, J. M. Lehn and J. Rimmer, *J. Chem. Soc., Dalton Trans.*, 1985, 1517 and refs. therein; P. J. Reddy, V. Ravichandran, K. K. Chacko, E. Weber and W. Saenger, *Acta Crystallogr., Sect. C*, 1989, **45**, 1871; M. E. Sobhia, K. Panneerselvam, K. K. Chacko, I.-H. Suh, E. Weber and C. Reutel, *Inorg. Chim. Acta*, 1992, **194**, 93; Y.-H. Lai, L. Ma and K. Mock, *Tetrahedron*, 1996, **52**, 4673.
- 5 C. O. D. Buchecker, J. M. Kern and J. P. Sauvage, *J. Chem. Soc., Chem. Commun.*, 1985, 760; C. O. D. Buchecker and J. P. Sauvage, *Chem. Rev.*, 1987, **87**, 795; C. O. D. Buchecker, J. M. Kern and J. P. Sauvage, *J. Chem. Soc., Chem. Commun.*, 1989, 760; J. P. Sauvage, *Acc. Chem. Res.*, 1990, **23**, 319; J. C. Chambron, D. K. Mitchell and J. P. Sauvage, *J. Am. Chem. Soc.*, 1992, **114**, 4625 and refs. therein.
- 6 Md. Athar Masood, R. Jagannathan and P. S. Zacharias, *J. Chem. Soc., Dalton Trans.*, 1991, 2553; Md. Athar Masood, D. J. Hodgson and P. S. Zacharias, *Inorg. Chim. Acta*, 1994, **99**, 221.
- 7 K. J. Takeuchi, M. S. Thompson, D. W. Pipes and T. J. Meyer, *Inorg. Chem.*, 1984, **23**, 1845; L. De Cola, F. Barigelletti, V. Balzani, P. Belser, A. von Zelewsky, F. Vögtle, F. Ebmeyer and S. Grammenudi, *J. Am. Chem. Soc.*, 1988, **110**, 7210; V. Balzani, F. Barigelletti and L. De Cola, *Top. Curr. Chem.*, 1990, **158**, 31; K. Bierig, R. J. Morgan, S. Tysøe, H. D. Gafney and T. C. Streckas, *Inorg. Chem.*, 1991, **30**, 4898; J. P. Collin, M. Baley and J. P. Sauvage, *Inorg. Chim. Acta*, 1991, **186**, 91; Md. Athar Masood and D. J. Hodgson, *Inorg. Chem.*, 1993, **32**, 4839 and refs. therein.
- 8 J. M. Lehn, in *Supramolecular Chemistry, Concepts and Perspectives*, VCH, Weinheim, 1995.
- 9 A. J. Blake, F. Demartin, F. A. Devillanova, A. Garau, F. Isaia, V. Lippolis, M. Schröder and G. Verani, *J. Chem. Soc., Dalton Trans.*, 1996, 3705.
- 10 (a) F. Contu, F. Demartin, F. A. Devillanova, A. Garau, F. Isaia, V. Lippolis, A. Salis and G. Verani, *J. Chem. Soc., Dalton Trans.*, 1997, 4401; (b) A. J. Blake, R. O. Gould, T. I. Hyde and M. Schröder, *J. Chem. Soc., Chem. Commun.*, 1987, 1730, 431; (c) A. R. Brown, F. W. J. Mosselmans, S. Parsons, M. Schröder, K. J. Tayan and L. J. Yellowlees, *J. Am. Chem. Soc.*, 1998, **120**, 8805.
- 11 H. Gampp, M. Maeder, C. J. Meyer and A. Zuberbühler, *Talanta*, 1985, **32**, 95.
- 12 G. Crisponi and V. Nurchi, *J. Chem. Educ.*, 1989, **66**, 54.
- 13 S. Peng, J. A. Ibers, M. Millar and R. H. Holm, *J. Am. Chem. Soc.*, 1976, **98**, 8037; S. Peng and V. L. Goedkin, *J. Am. Chem. Soc.*, 1976, **98**, 8500; C. Godson, K. P. Healy and D. Pletcher, *J. Chem. Soc., Dalton Trans.*, 1978, 972; A. Bakac and J. H. Espenson, *J. Am. Chem. Soc.*, 1986, **108**, 713; M. S. Ram, A. Bakac and J. H. Espenson, *Inorg. Chem.*, 1986, **25**, 326.
- 14 J. Lewis and M. Schröder, *J. Chem. Soc., Dalton Trans.*, 1982, 1085.
- 15 M. C. Aragoni, M. Arca, G. Crisponi and V. M. Nurchi, *Anal. Chim. Acta*, 1995, **316**, 195.
- 16 G. M. Sheldrick, SHELXS 86–97, Programs for Crystal Structure Solution, University of Göttingen, 1986–1997.
- 17 G. M. Sheldrick, SHELXL 93–97, Programs for Crystal Structure Refinement, University of Göttingen, 1993–1997.
- 18 J. Cosier and A. M. Glazer, *J. Appl. Crystallogr.*, 1986, **19**, 105.
- 19 J. A. Darr, S. R. Drake, M. B. Hursthouse and K. M. A. Malik, *Inorg. Chem.*, 1993, **32**, 5704.
- 20 W. Clegg, *Acta Crystallogr., Sect. A*, 1981, **37**, 22.

Paper 8/08062C